Science of the Total Environment 984 (2025) 179726

Contents lists available at ScienceDirect

Science of the Total Environment

journal homepage: www.elsevier.com/locate/scitotenv

DNA index determination by flow cytometry and TEM imaging of the ultrastructure of L929 cells exposed to a Euro 6 diesel exhaust gas mixture in a Bio-Ambient-Tests chamber

Aleksandra Kęska [a,*], Michał Kulus [b], Katarzyna Haczkiewicz-Leśniak [b]

[a] Wroclaw University of Science and Technology, Department of Automotive Engineering, Wybrzeże Wyspiańskiego 27, 50-370 Wrocław, Poland
[b] Wroclaw Medical University, Department of Ultrastructural Research, T. Chałubińskiego 6a, 50-368 Wrocław, Poland

HIGHLIGHTS

- Exhaust gases can lead to mitochondrial damage and oxidative stress in cells.
- Engine idling promotes cell death and inhibits cell proliferation.
- Cells exposed to exhaust gases may be capable of anastasis.

GRAPHICAL ABSTRACT

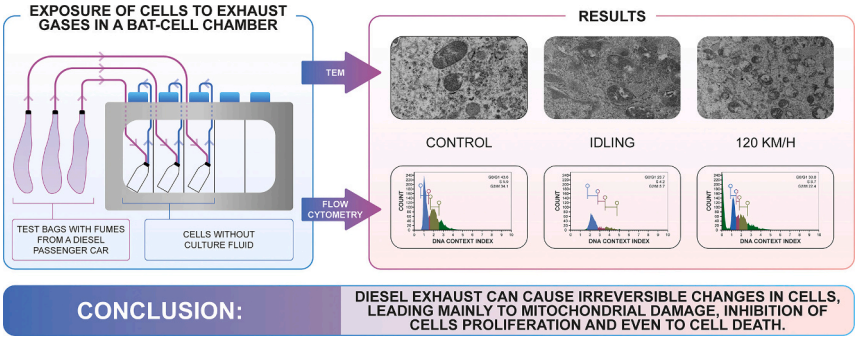

ARTICLE INFO

Editor: Henner Hollert

Keywords:
Internal combustion engine
Emission
Intercellular morphology
Cell death

ABSTRACT

Despite the development of electromobility, diesel engines still constitute a significant share of transportation. Given the complex composition of diesel exhaust emissions and their potential cytotoxic effects, it is crucial to investigate their impact on cellular structures to better understand their implications for human health. The aim of this study was to investigate the impact of a Euro 6 diesel exhaust gas mixture on L929 cells. The research was conducted using the BAT-CELL method, which allows for the direct exposure of cells to pollutants under controlled laboratory conditions. Flow cytometry was employed to analyze the cell cycle and determine viability of cells, while transmission electron microscopy (TEM) was used to assess the ultrastructure of the cells. The results revealed significant changes in cell structure and differences in proliferation and viability depending on the engine operating conditions. Notably, exposure to exhaust gases during idling and at a speed of 120 km/h led to significant mitochondrial damage and the activation of death processes. These findings provide important data on the cytotoxicity of diesel exhaust gases and may contribute to a better understanding of the impact of pollutants on human health.

* Corresponding author.
E-mail address: aleksandra.keska@pwr.edu.pl (A. Kęska).

https://doi.org/10.1016/j.scitotenv.2025.179726
Received 18 January 2025; Received in revised form 9 April 2025; Accepted 19 May 2025
Available online 24 May 2025

1. Introduction

Despite the development of electromobility (Koman et al., 2024), exhaust emissions from vehicles equipped with compression-ignition engines continue to be a subject of extensive research. The primary areas of focus include studies on the chemical composition of exhaust gases and its variability (Nabi et al., 2024), research on particulate matter and its characteristics (Ansari et al., 2024), new emission reduction technologies (Andrych-Zalewska et al., 2023), the impact of new biofuel blends on emissions (Kale and Krishnasamy, 2024) as well as the methods for monitoring emissions (Bortnowski et al., 2024) and their effects on human health (Kumar and Behera, 2024). Research on the cytotoxicity of exhaust emissions from engines is particularly important in the context of their impact on human health and the natural environment (Kęska et al., 2024). However, this issue is not sufficiently addressed in the literature. Such research involves assessing the direct impact of chemical substances contained in exhaust gases on living cells, including the cells viability, proliferation, and the exhaust gases potential to cause DNA damage. These studies allow for the identification of potential cellular-level threats that may lead to serious health conditions, such as cancer, respiratory diseases, and cardiovascular disorders.

In the context of environmental toxicology, cytotoxicity studies are significant because they allow for the assessment of the complex effects of the mixtures of substances present in exhaust gases, which may exhibit synergistic or antagonistic effects. Traditional emission tests, such as those required by the Euro emission standards, focus on the quantitative determination of specific pollutants but do not provide information on the actual impact of exhaust gases on living organisms (Kęska, 2023).

The Euro standards, introduced to limit the emission of harmful substances from motor vehicles, undoubtedly have a positive impact on air quality. These standards specify the maximum allowable concentrations for various compounds, such as hydrocarbons (HC), nitrogen oxides (NOx), carbon monoxide (CO), and particulate matter (PM). However, while the Euro 6 standards represent a significant step forward in emission reduction, they do not fully account for the complexity of exhaust gas interactions with human health. The emission tests upon which these standards are based are conducted under controlled laboratory conditions and focus on measuring specific substances under ideal conditions. In reality, road conditions, driving style, vehicle age, and chemical interactions in the atmosphere can significantly alter the toxicity of emitted exhaust gases. Moreover, the Euro standards do not consider the presence of numerous substances, interactions of which may lead to greater toxicity than the sum of the individual components. It has been repeatably scientifically proven that the toxicity of exhaust gases is determined by the hydrocarbons present in them. Among these, two particularly harmful groups of compounds stand out: polycyclic aromatic hydrocarbons (PAHs) and volatile organic compounds (VOCs), which can lead to carcinogenic changes and other serious health conditions (Fu et al., 2024; Li et al., 2023).

The L929 cell line, derived from mouse fibroblasts, is used as a model to study the cytotoxicity of various environmental factors, including engine exhaust gases (Kęska et al., 2022). Flow cytometry is a key tool in cellular toxicity studies, allowing for precise determination of the DNA index and analysis of the cell cycle, enabling the assessment of cell proliferation and death (Darzynkiewicz et al., 2010). Additionally, transmission electron microscopy (TEM) is invaluable for imaging the ultrastructure of cells, allowing for the identification of even subtle morphological changes at the organelle level (Zawadzka-Knefel et al., 2023). The use of the proposed methods in the study of the cytotoxicity of engine exhaust gases emitted from vehicles allows for a more comprehensive understanding of the effects of gas mixtures on living cells.

In this study, the impact of a mixture of exhaust gases from a diesel engine complying with Euro 6 emission standards on L929 cells was analyzed. The results obtained for different engine operating conditions were compared, allowing for the identification of harmful operating modes. The research was conducted using the advanced BAT-CELL method, which allows for direct contact of cells with the tested gas mixture under controlled laboratory conditions (Kęska et al., 2023). The findings are significant for assessing the health risks associated with exposure to pollutants from modern diesel engines, which are still widely used worldwide (Li et al., 2024; Rahman Adib et al., 2024).

2. Materials and methods

2.1. Research object

The tests covered exhaust gases emitted from a Volkswagen Passat Limousine 2.0 TDI passenger vehicle equipped with a diesel engine. The technical parameters of the vehicle are presented in Table 1. The vehicle has passed a technical inspection at a vehicle inspection station. An additional inspection was carried out at the testing site in order to ensure no defects of the vehicle. The inspection included a visual assessment of the engine compartment for leaks or irregularities in the operation of power unit components and for the tightness of the exhaust system.

The vehicle was approved before 2017 during the period of validity of the Euro 6 standard in the version D. The vehicle was powered by commercially available Ekodiesel ULTRA diesel oil with a biocomponent content not exceeding 7 %.

2.2. Method of exhaust gas sampling

The collection of exhaust gases emitted from the vehicle was carried out on the MAHA MSR 1050 chassis dynamometer. The test station, due to its ability to generate braking and driving torque, allows for simulating the vehicle's movement resistance. In order to determine the vehicle's movement resistance (rolling and air resistance coefficients), a coastdown test was performed. The vehicle's inertial resistance was determined by measuring the actual vehicle mass. The inertia component in this case was negligible, measurements were carried out for a constant vehicle speed. Data from the tests was implemented into the test station's software, which, through the appropriate distribution of torque, simulated the vehicle's motion resistance during operation in real conditions. Before the main measurements have been performed, the external characteristics of the vehicle were determined.

The tests were carried out in four vehicle states: while stationary (engine idling), while driving at a speed of 50 km/h, and at 120 km/h (drive system ratio according to the gearbox control algorithm) and during forced DPF (Diesel Particular Filter) regeneration by Bosch KTS diagnostic software.

Each time, the engine and drive system were running at a temperature typical for a given condition. The conditions were met by maintaining the vehicle at a defined operating point for a period of 15 min before the start of the tests until the vehicle's thermal equilibrium was achieved.

To collect exhaust gases, a silicone pipe with a metal extension was placed in the vehicle's exhaust pipe. The other end was connected to an

Table 1
Technical parameters of a vehicle with a diesel engine.

Fuel type	Ekodiesel ULTRA
Displacement engine	1968 cm^3
Maximum power	110 kW at 3500 rmp
Maximum torque	340 Nm at 1750–3000 rpm
Actual vehicle weight	1475 kg
Drive type	4 × 2
Gearbox type	Manual, 6 gears
Year of production	2017
Exhaust emission level	EURO 6D
Vehicle mileage	88520 km

inert sampling bag placed in a special aspiration system.

For each vehicle condition, exhaust gases were collected into two prepared bags with a capacity of 10 dm^3 in order to examine exhaust gas toxicity in in vitro tests. During sampling, the emission level of harmful exhaust gas components was monitored using an automatic exhaust gas analyzer MAHA MET 6.1, equipped with an NDIR (Non Dispersive Infra Red) infrared sensor to monitor the concentration of carbon monoxide, carbon dioxide and hydrocarbons, and an electrochemical oxygen sensor.

2.3. Cell culture

The research used the adherent fibroblast-like cell line L929 (ECACC 85011425) obtained from the subcutaneous adipose tissue of mice, which can be used for toxicity testing. This line is a reference model used in the assessment of the cytotoxicity of biomaterials in accordance with the ISO-10993:5 standard (ISO-10993:5, Biologiczna ocena wyrobów medycznych – Część 5: Badania cytotoksyczności in vitro, n.d.).

2.3.1. Carrying out a cell culture

Cell culture was carried out using standard operating procedures (Paduch, 2019). The culture was carried out in MEM (Minimum Essential Medium) with Earle's Salts (Capricorn Scientific, Ebsdorfergrund, German) enriched with 10 % fetal bovine serum (FBS, Sigma-Aldrich, St. Louis, MO, USA) and 1 % L-glutamines, penicillin, streptomycin, and an acidity regulator HEPES (Sigma-Aldrich). The culture was carried out in a humid atmosphere under standard conditions: 37 °C, 5 % CO_2 in a CELL 50 Comfort S CO_2 incubator. Cells were passaged using 0.25 % trypsin-EDTA solutions (Sigma-Aldrich) at 70 % confluence. The cells used for the analysis were at passages 12–14. Control imaging of cells during culture was performed using an AE31E trino inverted microscope with a maximum magnification of 400 times, equipped with a Moticam Pro S5 Lite camera.

2.3.2. Exposure of cells to exhaust gases

Twenty four hours before exposure to exhaust gases, cells were seeded into bottles with adherent medium with an area of 25 cm^2 at a density of 28,000 cells/cm^2. Cells were quantified using an Eve™ NanoEn Tek Inc. automatic cell counter.

The BAT-CELL Bio-Ambient-Tests method (patent, PL, No. 220670) was used to expose cells to a mixture of exhaust gases. The method enables the assessment of the toxic effect of gas mixtures on the health of living organisms. The prepared cell line, devoid of culture fluid, is placed in a sterile sampler. Then, the aspiration system draws exhaust gases into the sampler through an inlet pipe equipped with an antibacterial filter that acts as a barrier to particulate matter. After exposure, the cells are flooded with culture fluid and the direct effect of toxic gases on living cells is examined using toxicological tests, for instance a viability test. The exposure time is selected individually depending on the type of gas mixture being tested. For exhaust gases, the exposure time was set to 7.5 min (Kęska et al., 2022). The flow parameters were adjusted to the shape of the sampler in such a way as to enable uniform contact of the gas particles with the cell surface and not to damage them mechanically. The flow rate of tested gases through the aspiration system was set at 150 cm^3/min (Kęska et al., 2023).

The conditioning chamber (Fig. 1) in which the samplers were placed was equipped with pressure and temperature sensors to ensure that the vital functions of the cell culture had been maintained. Elimination of the culture fluid was possible due to maintaining physical parameters, adjusted to the requirements of a given cell line, safe for the cells outside the incubator atmosphere for a specified period, and without the supply of nutrients. The cell line sampler was additionally protected at the inlet with an antibacterial filter. Three samples were exposed to each of the prepared simulated vehicle conditions and three control tests were carried out: a sampler with cells left in the laboratory, a sampler with cells exposed to vehicle ambient air (background) and a sampler without gas flow left in the BAT-CELL chamber.

The repeatability of the BAT-CELL Bio-Ambient-Tests method was estimated at the level of 5 %, which is a relatively low value compared to other biological methods (Janicka, 2013). The method error is related to the average reading error value from the tested samples and was determined during previous experiments.

2.4. Flow cytometry

Forty eight hours after exposure to the exhaust gas mixture (Kęska et al., 2022), the cells were subjected to cytotoxicity tests conducted with flow cytometry. DNA content index (DI) in cells at different phases of the cell cycle was measured using the Muse Cell Cycle kit and the Guava Muse cell analyzer (Cytek Biosciences). The measurement results are presented in the form of histograms and the percentage of cells in the main phases of the cell cycle. The percentage values of the coefficient of variation for individual samples (CV%) were determined. Muse 1.9.1 Analysis software was used to process the data. In addition, cells were counted using the Muse Count & Viability kit. The total number of cells and the number of living cells were counted. Cell survival was presented as the percentage of viable cells relative to percentage of viable cells in the laboratory control. Both analyses were performed according to the manufacturer's recommended protocols (Luminex Corporation).

2.5. TEM imaging

Four samples were selected for preparation and imaging, including a laboratory control sample, samples after exposure to exhaust gases

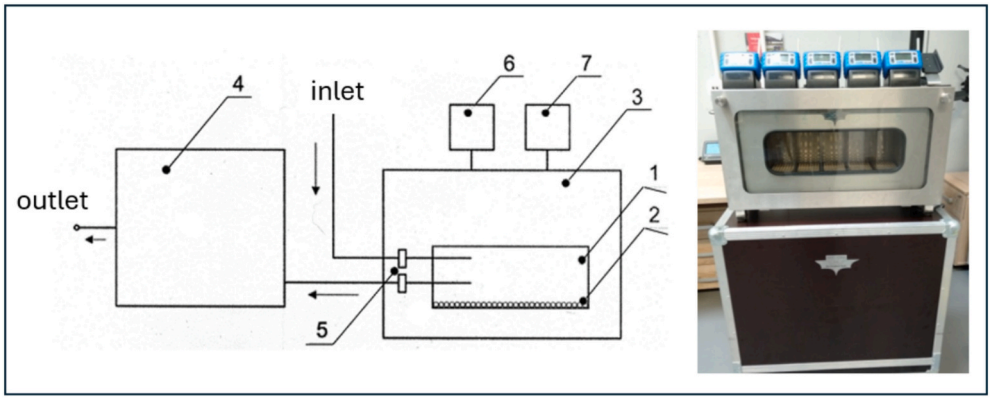

Fig. 1. A measurement system of gas toxicity evaluation by BAT-CELL (1 – cell sampler, 2 – cells without culture fluid, 3 – BAT-CELL chamber, 4 – aspirator, 5 – antibacterial filters, 6 and 7 – temperature and pressure sensors).

emitted: at idle speed, while driving at 120 km/h, and during forced DPF regeneration. Cells were processed as described before (Solarska-Ściuk et al., 2022). After 48 h exposure to the exhaust gas, the cells were treated with trypsin, washed in phosphate-buffered saline (PBS), and centrifuged (800 rpm, 5 min) to obtain pellets. Subsequently, the pellets were fixed in glutaraldehyde at room temperature (3.6 %, 25 min, SERVA Electrophoresis, Heidelberg, Germany). Subsequently, the fixative was removed by washing with 0.1 M cacodylate buffer (SERVA Electrophoresis) and distilled water during centrifugation (1800 rpm, 8 min). Later, the cell pellets were entrapped into the fibrin clot, which had been prepared by combining 0.05 mL of bovine plasma thrombin (500 units of lyophilized powder solubilized in PBS; Sigma-Aldrich, Merck KGaA, Darmstadt, Germany) with 0.1 mL of fibrinogen (1 mg/mL; Merck KGaA, Darmstadt, Germany).

The post-fixation of the samples was conducted for one hour using osmium tetroxide (1 %, v/v) dissolved in cacodylate buffer (Agar Scientific, Stansted, Essex, UK). Subsequently, the samples were rinsed with 0.1 M cacodylate buffer for a period of three minutes, three times. They were then dehydrated in increasing concentrations of ethanol, from 30 % to 100 %, then in a mixture consisting of 90 % ethanol and 90 % acetone. Finally, they were dehydrated in graded acetone concentrations, 90 %, 95 %, and 100 %. Subsequently, the samples were infiltrated with a mixture of epoxy resin (Epon 812, SERVA Electrophoresis) and acetone. The samples were embedded in capsules (embedding molds; Pelco, Ted Pella, Redding, CA, USA) using an epoxy resin consisting of glycid ether, methylicanhydric, and dodecenyl succinic anhydride in a 3:1 ratio for 20 min, then in a 1:1 ratio for 60 min, and finally in a 1:3 ratio for a further 60 min.

The cutting procedure entailed the preparation of semi-thin sections (600 nm) and ultrathin sections (70 nm) on the RMC ultramicrotome (Power Tome XL; Tucson, AZ, USA) with a diamond knife (Diatome, Nidau, Switzerland) derived from the epoxy blocks. The semi-thin sections were stained at 100 °C with 1 % toluidine blue (SERVA Electrophoresis). Rhodium-copper grids (200 mesh, Maxta form, Ted Pella, Redding, CA, USA) with the ultrathin sections were counterstained with the lantanides solution (Uranyless, Mauressac, France) and 3 % Reynold's lead citrate (Electron Microscopy Sciences, Hatfield, PA, USA) and then rinsed five times in ultrapure water (Millipore, Milli-Q® Reference system, Merck KGaA, Darmstadt, Germany).

The counterstained sections were observed with a transmission electron microscope (JEM-1011, JEOL, Tokyo, Japan) and imaged with a Morada camera (Olympus, Münster, Germany).

3. Results

3.1. Cytotoxicity tests

3.1.1. Cell cycle analysis of DNA

Measurement of DNA content using flow cytometry was performed to estimate the frequency of cells in different phases (G0/G1 versus S versus G2/M) of the cell cycle. Fig. 2 shows the population profile for the control and representative experimental samples. The entire population profile was analyzed. The profiles for the control samples: laboratory control and without flow, as well as for the speed of 50 km/h and with DPF, appear comparable. The background profile is similar to the profile for the speed of 120 km/h. A significant number of damaged cells with DI < 1 values are observed. The profile for idling, compared to the other profiles, is characterized by a lower cell count.

Fig. 3 shows the DNA content profile histograms. The gates on the histograms were set in a specific manner (Darzynkiewicz et al., 2010). The blue gate for the G0/G1 phase includes the first peak. The second purple gate defines the S phase. The third green gate for the G2/M phase includes the second peak. The percentage of cells in each phase of the cycle is noted in the upper right corner of the histograms.

Table 2 summarizes the calculated values for damaged cells, apoptotic sub-G1 cells, proliferating G0/G1 cells, cells in the S phase of the increase in the amount of DNA, G2/M cells with double genetic material, and polyploid cells. The table also includes the coefficients of

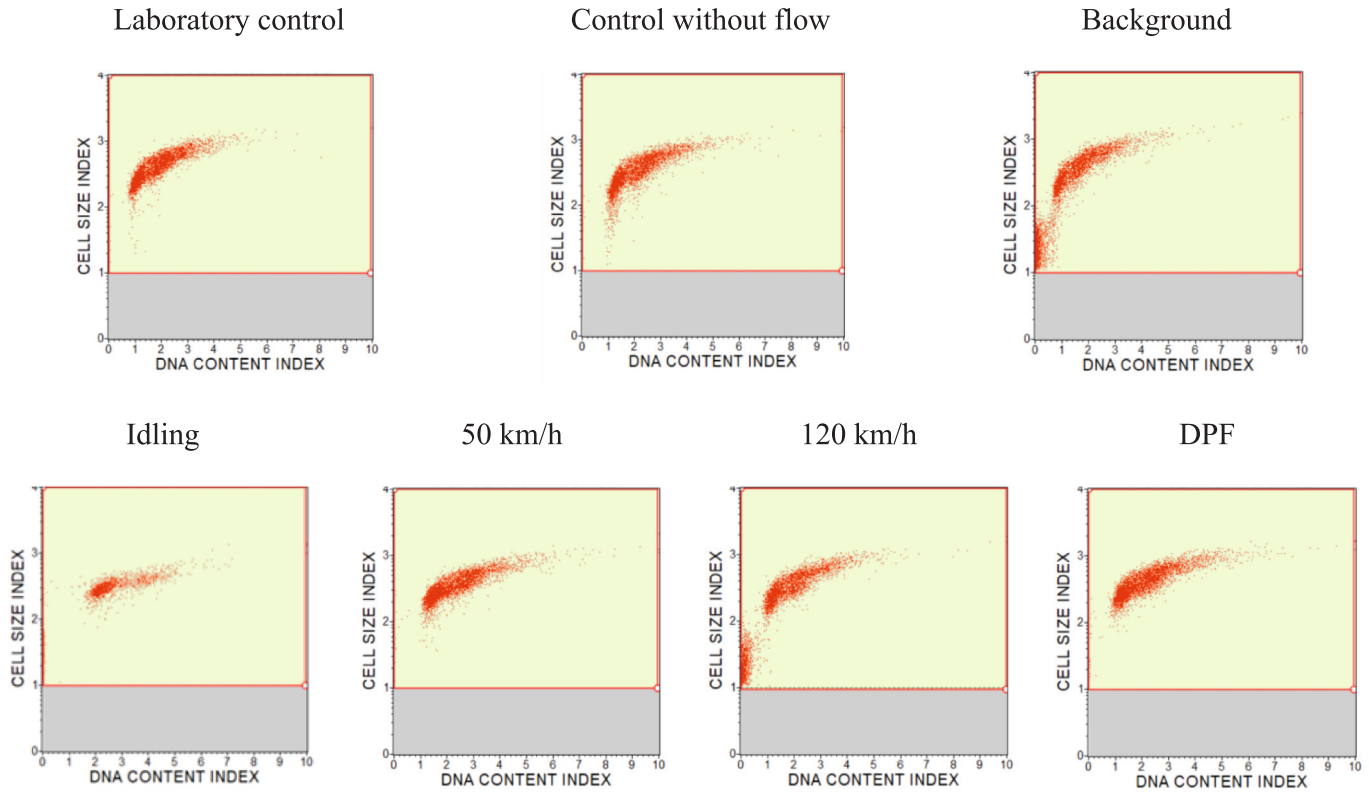

Fig. 2. Cell cycle analysis of DNA - population profile.

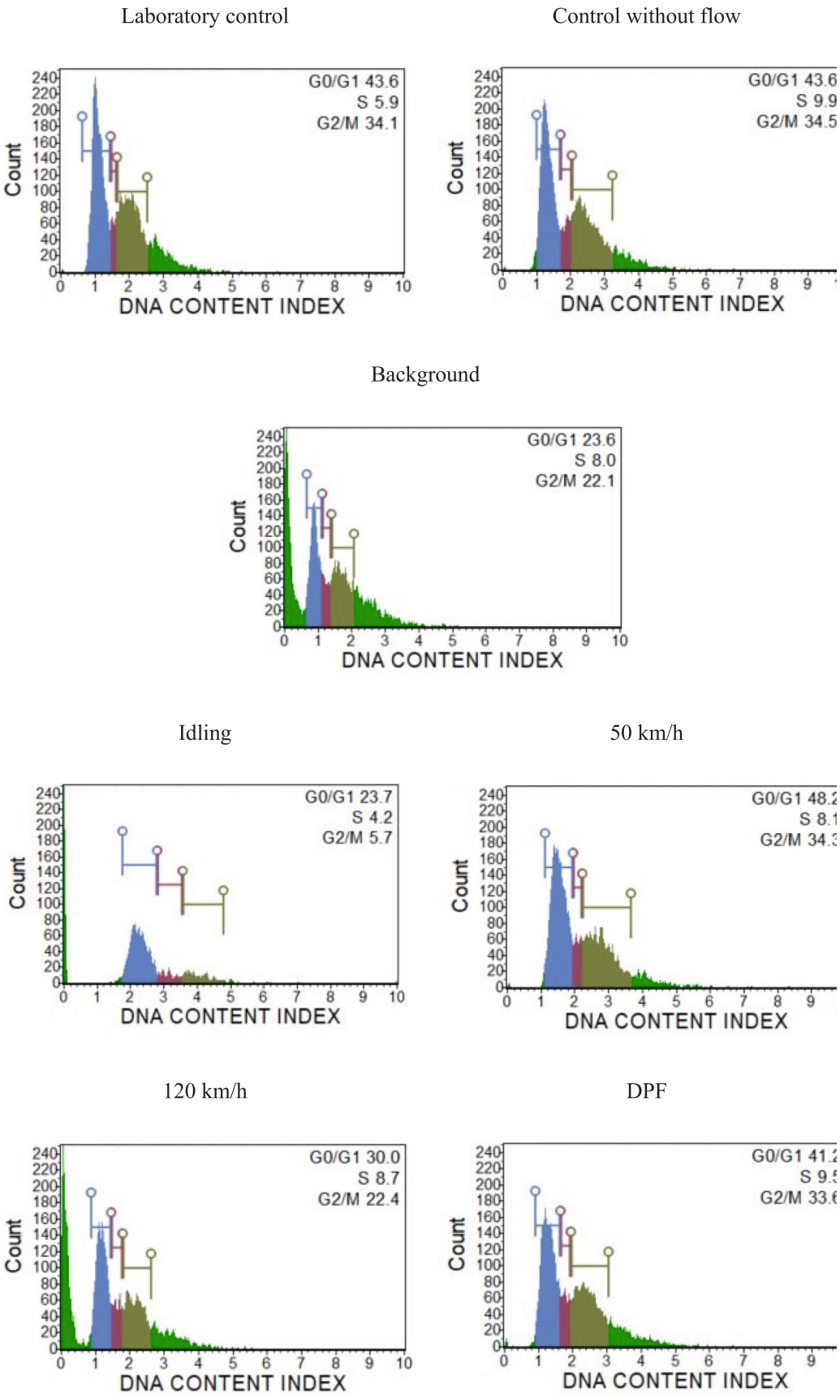

Fig. 3. Cell cycle analysis of DNA – DNA content profile.

Table 2
Percentage of cells in selected phases of the cell cycle.

Samples	%sub-G1	%G0/G1	%CV	%S	%CV	%G2/M	%CV	%Poliploidy
Laboratory control	0.4	43.6	13.9	5.9	3.4	34.1	11.6	16.0
Control without flow	1.7	43.6	12.4	9.9	5.1	34.5	12.6	10.3
Background	26.6	23.6	12.7	8.0	6.5	22.1	11.1	19.7
Idling	65.8	23.7	10.7	4.2	6.7	5.7	8.1	0.6
50 km/h	1.2	48.2	12.9	8.1	3.8	34.3	13.2	8.2
120 km/h	25.1	30.0	11.6	8.7	5.9	22.4	10.2	13.8
DPF	1.2	41.2	13.5	9.5	4.8	33.6	12.1	14.5

variation (%CV) values for main phases. There is no formal arrangement for an acceptable maximum %CV of the average DNA content of cell population, i.e., an acceptable error in estimating the DNA content of cells (Darzynkiewicz et al., 2010). The highest percentage for sub-G1 and the lowest for G0/G1 were recorded in the following samples: idling, background, and 120 km/h. Reduced percentage values for the G2/M phase were noted for the samples: idling (only 5.7 %), background (22.1 %) and 120 km/h (22.4 %). The lowest percentage value in the S phase was recorded in the control laboratory sample and for idling. The percentage of polyploid cells was also calculated. For the 50 km/h sample, the percentage of polyploid cells (8.2 %) was half of the control laboratory sample (16.0 %). The %CV values for the G0/G1 phase ranged between 10.6 % and 13.9 %, for the S phase ranged between 3.4 % and 6.7 %, for the G2/M phase ranged between 8.1 % and 13.2 %.

3.1.2. Viability of cells

The cell cycle study results revealed a low cell count for the idling sample. This was confirmed by the cell viability test conducted using flow cytometry. Research data are presented in Table 3. Three repetitions were performed for the samples exposed to engine exhaust gases.

Fig. 4 shows the average percentage of total cells after exposure to engine exhaust compared to the laboratory control. The lowest total cell count was recorded for idle running, which was 22 % lower than in the laboratory control. Additionally, the percentage of living cells is marked with green and the percentage of dead cells with red.

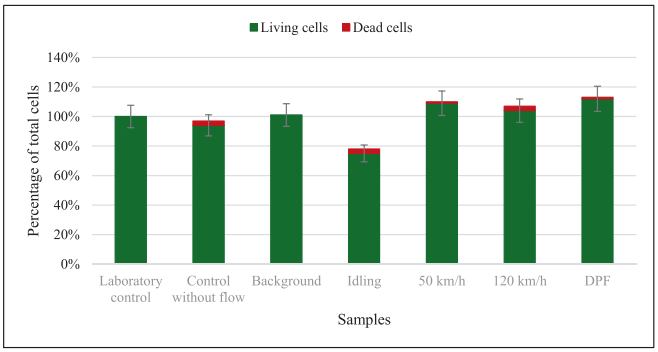

Fig. 4. Average percentage of total cells 48 h after exhaust gases exposure.

Table 3
Flow cytometer data and calculated.

Samples	Total cells/ml [×10^6]	Live cells/ml [×10^6]	Viability	Viability vs laboratory control viability		Total cells vs total cells in laboratory control	
Laboratory control	3.10	3.03	98 %	100 %		100 %	
Control without flow	3.00	2.86	95 %	98 %		97 %	
Background	3.12	3.05	98 %	100 %		101 %	
Idling	2.21	2.08	94 %	96 %	97 %	71 %	
	2.45	2.35	96 %	98 %		79 %	78 %
	2.56	2.41	94 %	96 %		83 %	
50 km/h	3.13	3.02	96 %	99 %	100 %	101 %	
	3.50	3.42	98 %	100 %		113 %	110 %
	3.58	3.51	98 %	100 %		115 %	
120 km/h	2.95	2.83	96 %	98 %	98 %	95 %	
	3.60	3.51	98 %	100 %		116 %	107 %
	3.37	3.13	93 %	95 %		109 %	
DPF	3.52	3.42	97 %	99 %	100 %	114 %	
	3.43	3.35	98 %	100 %		111 %	113 %
	3.52	3.44	98 %	100 %		114 %	

3.2. Imaging of cells

The ultrastructure of cells was evaluated using transmission electron microscopy. Cells general morphology is compared in Fig. 5 and detailed ultrastructure – in Fig. 6. Control cells (Fig. 5A, B) exhibit a normal morphology that is typical for cultured mouse fibroblast cells. The nucleus (Nu) displays clear, mostly euchromatic nucleoplasm, with one or two nucleoli. The cytoplasm contains numerous normal organelles, including proper mitochondria. General morphology of cells exposed to idle exhaust gases (Fig. 5C, D) is similar to control cells, however some of them contain large vacuoles (V) (Yu et al., 2024). Some cells show increased amount of multivesicular bodies (mvb). The morphology of cells exposed to exhaust fumes emitted during driving at 120 km/h (Fig. 5E, F) shows similar morphology to cells exposed to exhaust fumes from idling. However, cellular debris (Necr) is more often observed. Some nuclei have irregular shape. The morphology of cells exposed to exhaust gases emitted during DPF filter combustion (Fig. 5G, H) is similar to that of the control sample.

At higher magnifications, more pronounced differences become evident (Fig. 6). The cytoplasm of control cells (Fig. 6A, B) is normal, lot of vesicles (ves) and some Golgi Apparatuses (GA) are visible. Rough endoplasmic reticulum (RER) is regular, slightly dilated in some cells. Mitochondria (mt) tend to be properly formed, some of them showing slightly damaged cristae. Cells exposed to idle exhaust fumes (Fig. 6C, D) show more damaged mitochondria. RER shows similar morphology as in control cells. Autophagic vacuoles (af) with visible lamellar bodies inside suggest ongoing mitophagy (Chakraborty et al., 2020). There are large vacuoles (V/mvb), which may be a result of merging large amount of multivesicular bodies. The size of the particles accumulated in the vacuoles ranges approximately from 75 to 150 nm. In cells exposed to exhaust fumes emitted while driving at 120 km/h (Fig. 6E, F), mitochondrial damage is extensive and widespread. RER tend to be more dilated than in previous cell lines. Vacuoles tend to be large and

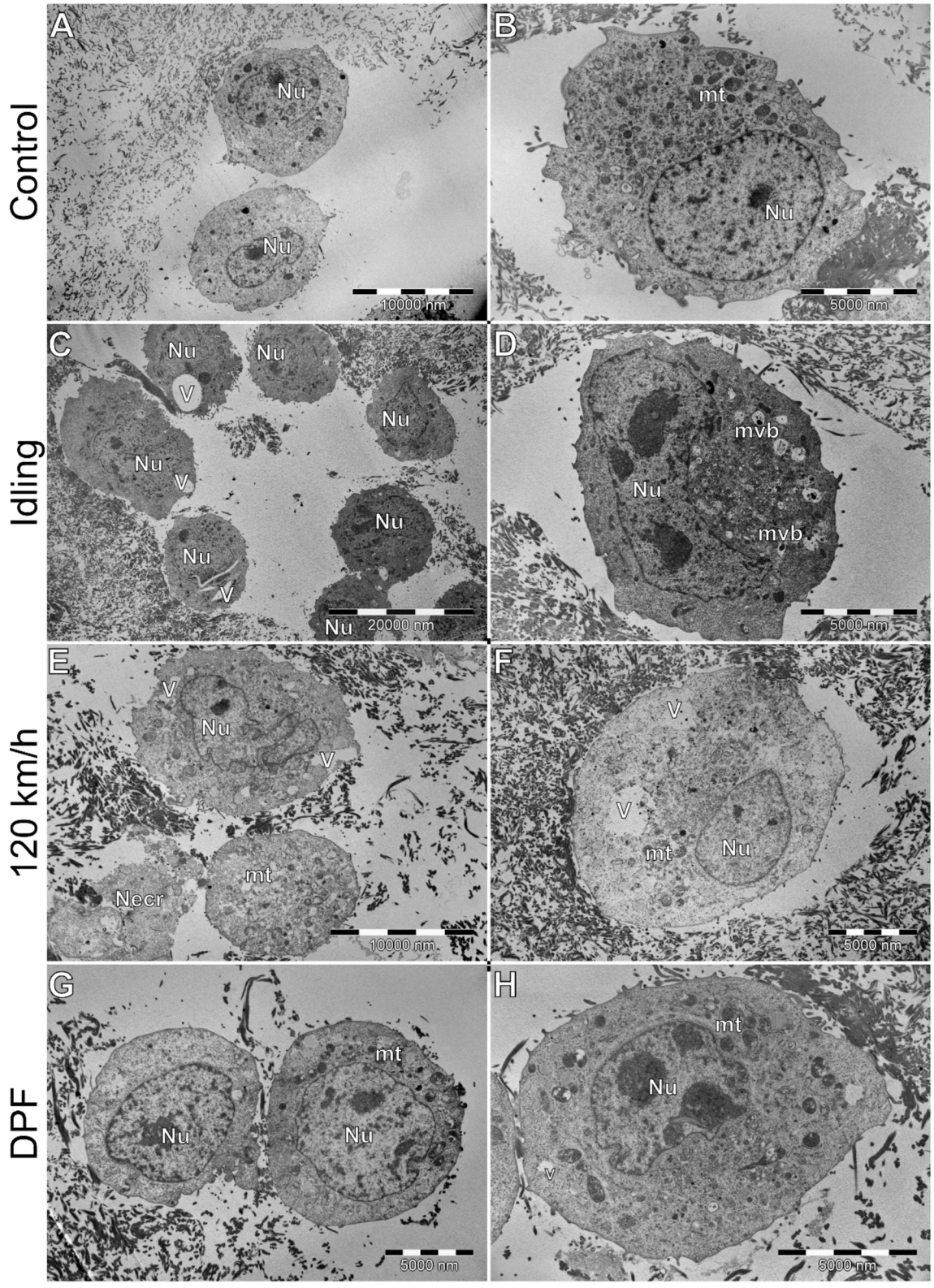

Fig. 5. A comparison of the general morphology of cells cultured under disparate conditions; A, B: The morphology of the untreated cells is unremarkable. The cell nuclei (Nu) are clear and round, and predominantly euchromatic. The mitochondria (mt) are clustered and appear normal. There is no evidence of significant damage. C, D: Cells exposed to fumes from idling tend to exhibit slight alterations, with the presence of large vacuoles (V) in some instances. In other cases, a considerable number of multivesicular bodies (mvb) can be observed. E,F: Cells exhibit a notable distortion in shape of their nuclei. The presence of vacuoles is more prevalent, and necrotic debris (Necr) is frequently observed. G, H: The introduction of DPF enables the cells to retain a morphology that closely resembles that of the untreated cell lines; Nu – nucleus, mt – mitochondria, mvb – multivesicular bodies, Necr – necrotic, cellular debris, V – vacuoles.

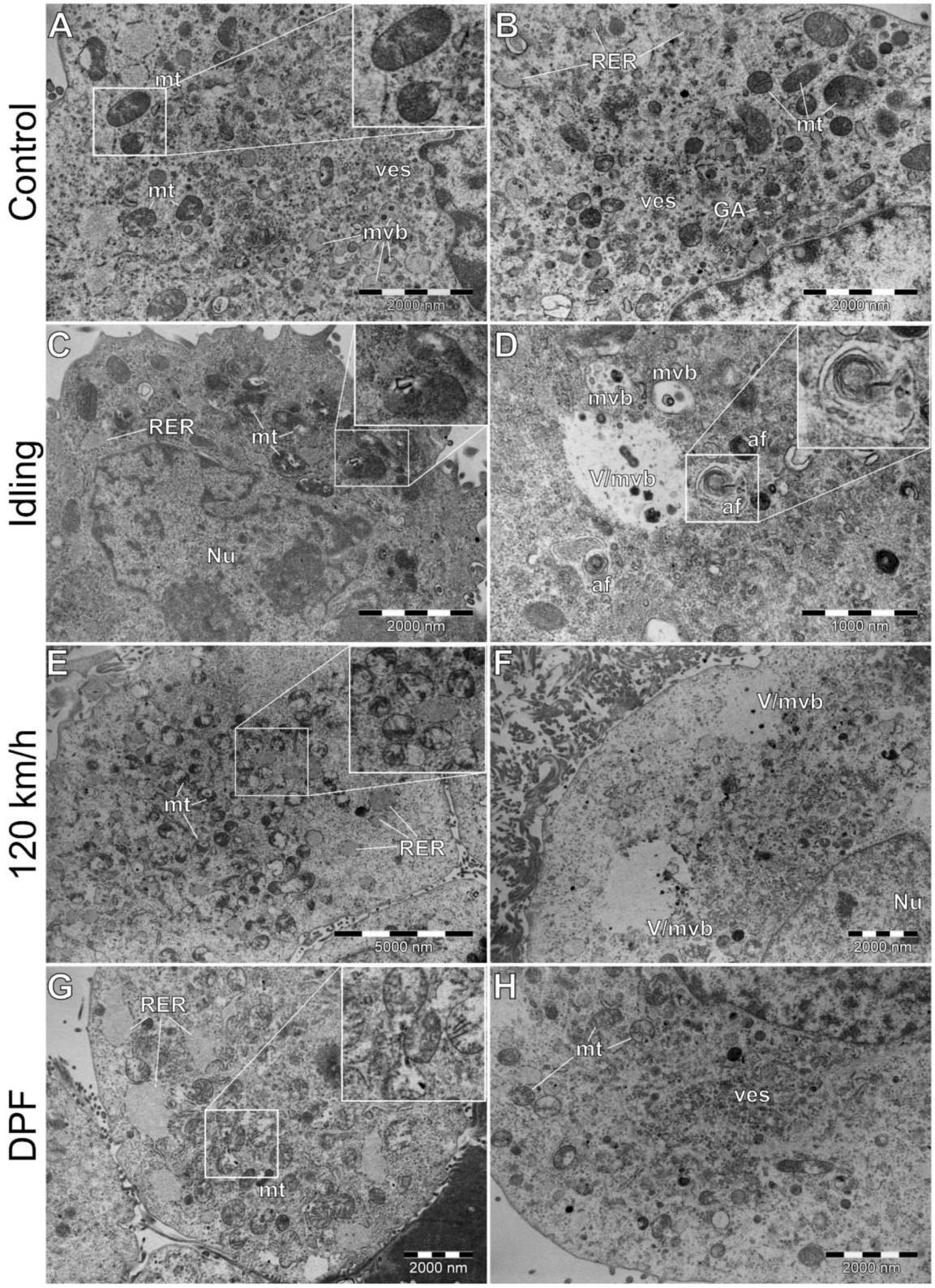

Fig. 6. Comparison of ultrastructural detail of cells cultured in different conditions; A, B: The majority of organelles in the untreated cells are intact. However, a minor proportion of mitochondria exhibit evidence of damage. C, D: The damage to the mitochondria is more prevalent and pronounced. Some autophagic vacuoles (af) with lamellar mitochondrial debris can be observed, as well as dilated rough endoplasmic reticulum (RER) E, F: The majority of mitochondria are severely damaged, and ruptured vacuoles or multivesicular bodies (MV/MVB) are commonly observed. The size of the particles accumulated in the vacuoles ranges approximately from 75 to 150 nm. Dilated rough endoplasmic reticulum (RER) is clearly visible. G, H: The ultrastructure of the organellae is comparable to that observed in specimens exposed to fumes from idling; Nu – nucleus, mt – mitochondria, mvb – multivesicular bodies, Necr – necrotic, cellular debris, V/mvb – vacuoles, possibly multivesicular bodies, af – autophagosomes, ves – vesicles, GA – Golgi Apparatus.

damaged. Dilated RERs are visible in cells exposed to exhaust gases emitted during DPF filter combustion (Fig. 6G, H). Mitochondrial damage is similar as in cells exposed to idle exhaust fumes.

4. Discussion

In the current study, cell number, viability, cell cycle stage and ultrastructure were compared when cultured in exposure to different exhaust gases. Cell number and viability were lowest in the idling group and slightly increased in all other groups. Cell cycle analysis and measurement of DNA content with cytometry revealed differences in cell numbers at different stages of the cycle, particularly in the idling sample, where the lowest cell number was observed. A high percentage of sub-G1 cells indicated a high prevalence of cell death in this group. However, ultrastructural analysis revealed the most damaged mitochondria in the 120 hm/h group, whereas mitochondrial damage was less pronounced in the idling and DPF groups.

Differences in cell viability and ultrastructure are most likely caused by the different composition of the exhaust gases under different driving conditions. Idling tends to exhibit high levels of aromatics and non-methane hydrocarbons. As the engine speed increases, the proportion of aromatics decreases, the proportion of alkanes increases, and the proportion of non-methane hydrocarbons decreases (Zhang et al., 2020).

Increased cell count in the 50 km/h, 120 km/h, and DPF group is somewhat surprising, but consistent with previous results. In study by Landwehr et al., exhaust from some fuels similarly resulted in increased cell count (Landwehr et al., 2021), other studies show no differences in cell viability when exposed to gas exhaust (Bisig et al., 2015). In vivo studies on wound regeneration shows that carbohydrates and their derivatives may be actually used to amplify cell proliferation rate (de Albuquerque et al., 2023).

However, despite slightly increased cell proliferation, ultrastructural analysis revealed damage, which could be indicative to occurrence of oxidative stress (Cole et al., 2010; Jendrach et al., 2008; Wu et al., 2024) in the cells exposed to gas exhaust, more pronounced in 120 km/h group than in the idling group. General cells morphology was not significantly affected. Cell shape remained unchanged regardless of the degree of exposure to exhaust gases. However, some cells exposed to exhaust gases showed the presence of large vacuoles, which may be the result of fusion of several multivesicular bodies or fusion or dilation of other vesicles (Wan et al., 2020). In the group most exposed to exhaust gases (120 km/h), some cellular debris is visible, suggesting apoptotic and/or necrotic cell death.

The organelles of the cells are more affected and show some features of oxidative stress (Collins et al., 2021). However, it must be acknowledged that oxidative stress cannot be definitively confirmed without additional methods. In particular, cells exposed to exhaust gases tend to have more damaged mitochondria (Fig. 6C–H). In some cells, autophagic vacuoles appear, with lamellar remains inside, indicating mitophagy (Wu et al., 2024). In the group most exposed to exhaust gases (120 km/h), the integrity of some vacuoles is broken and mitochondria are often swollen, as is the rough endoplasmic reticulum. Cells exposed to exhaust gases emitted during DPF regeneration show similar ultrastructure to the cells exposed to exhaust gases emitted engine idling. Occurrence of oxidative stress as a result of exposition to engine exhaust was confirmed also in previous studies (Bisig et al., 2015; Scholten et al., 2021). Study by Cattani-Cavalieri et al. (2024) demonstrated that diesel exhaust particles alter mitochondrial bioenergetics, leading to disruption of mitochondrial network and function, ultimately triggering mitophagy. In the current study, visible distortion of cell nuclei shape was observed, which may correspond with increased polyploidy rate (Mosieniak et al., 2015), evidenced by flow cytometry (Fig. 3).

Cells exposed to exhaust tend to show increased intracellular vacuolization. As previously demonstrated (Steiner et al., 2016), particles from diesel exhaust are often accumulated in cytoplasmic vacuoles. In the current study, electron-dense particles ranging from 75 to 150 nm were found inside vacuoles. It is plausible – although not certain – that these were exhaust particles, and particles within this size range are the most likely to be incorporated by cells.

This study highlights the importance of relying not only on cell viability, but also on cells quality in similar studies. Although the proliferation rate is slightly increased in cells exposed to fumes from the 120 km/h test drive, the oxidative stress is also increased. Both phenomena may result in increased carcinogenesis risk (Mandal, 2017).

Research shows that reduced cell viability after exposure to engine exhaust gases emitted at idle speed may be caused by the polycyclic aromatic hydrocarbons present in them. The more diverse the qualitative and quantitative composition of hydrocarbons, the more cells degenerate (Kęska et al., 2022). It is also possible that the decrease in cell viability may be caused by exposure to particulate matter contained in exhaust gases (Zerboni et al., 2022). It activates pro-inflammatory and carcinogenic pathways in the body (Botero et al., 2020; Niu et al., 2020).

Methods used in the current study could not indicate molecular pathways affected by diesel exhaust, but our observations correspond with biochemical changes reported in different studies. According to metabolomic studies, diesel exhaust change alanine and glutamine metabolism, mitochondrial carnitine shuttling, glutathione biosynthesis as well as sirtuin, and TP53 pathway (Chen et al., 2025), which could be one of the factors responsible for the changes in cell proliferation observed in the current study. Changes in mitochondria correspond with finding of Sivakumar and Kurian (2022), where diesel exhaust decreased the activity of electron transport chain proteins in mitochondria, as well as activity of catalase and superoxide dismutase, which could eventually lead to oxidative stress and cellular damage. Transcriptomics indicate on increase in expression of hypoxia-related genes and cell cycle and MAPK/ERK-related pathways (MAP3K2, MBIP, MAPK8, RRM2B, TBK1, ETS2, DUSP11, CAD) after exposure to diesel exhaust (Drizik et al., 2020). These biochemical changes lead to disruption of cell proliferation and mitochondrial structure and function – which corresponds with the results obtained in the current study.

In turn, the better proliferation capacity of cells exposed to exhaust gases from an engine operating under load may result from the cells' capacity of anastasis. This means the recovery of cells from the brink of apoptotic death. Such cells, although they may be genetically unstable and mutationally burdened, may have the capacity to proliferate (McDonald et al., 2021). This would explain the significant changes that occurred in the internal morphology of cells exposed to exhaust gases emitted while driving at a speed of 120 km/h and the simultaneous ability of these cells to proliferate better.

5. Conclusions

The following research indicates the harmful impact of exhaust emissions from the tested vehicle, equipped with a compression ignition engine, on living cells by disrupting their homeostasis. Exposure of L929 cell lines to exhaust gases can lead to:

- disruption of cellular organelle integrity, including mitochondrial damage, activation of mitophagy and oxidative stress.
- cell death through apoptosis and/or necrosis, particularly during engine idling.
- inhibition of cell proliferation during engine idling.

The cytotoxicity studies of engine exhaust gases using the BAT-CELL method take into account the actual impact of exhaust gases on living organisms. In these studies, the gas mixture is treated as a whole, and the phenomenon of additive synergism of compounds is also considered, where their mutual interaction can, for example, amplify the toxic effect of the entire gas mixture. Such studies can complement the currently performed emission tests for vehicles approved for road use. In addition to knowing the concentration values of individual compounds, as

specified in commonly applicable emission standards, such as Euro standards, it is crucial to understand the actual impact of exhaust gases on the human body.

CRediT authorship contribution statement

Aleksandra Kęska: Writing – original draft, Software, Resources, Project administration, Methodology, Investigation, Funding acquisition, Formal analysis, Data curation, Conceptualization. **Michał Kulus:** Writing – original draft, Visualization, Software, Methodology, Investigation, Formal analysis, Data curation. **Katarzyna Haczkiewicz-Leśniak:** Writing – review & editing, Supervision, Methodology.

Funding

The research was carried out thanks to funding from the Miniatura grant (2023/07/X/ST10/00090, National Science Centre, Poland) and partially funded by the research task *Imaging of cytotoxic effects induced by exposure to engine exhaust fumes*, financed from the pro-quality subsidy for the development of the research potential of the Faculty of Mechanical Engineering of the Wroclaw University of Science and Technology in 2024 (MPK 9100560000/8211204601, 8213204602).

Declaration of competing interest

The authors declare that they have no known competing financial interests or personal relationships that could have appeared to influence the work reported in this paper.

Acknowledgments

Authors thanks Agnieszka Szulak and Radosław Włostowski from Wroclaw University of Science and Technology as well as Magdalena Baran-Pelc from Wroclaw Medical University for research technical support. A.K. thanks Andrzej Żak from Wroclaw University of Science and Technology for inspiration and valuable advice.

Data availability

Data will be made available on request.

References

Andrych-Zalewska, M., Chlopek, Z., Pielecha, J., Merkisz, J., 2023. Influence of the in-cylinder catalyst on the aftertreatment efficiency of a diesel engine. Energies (Basel) 16, 2826. https://doi.org/10.3390/en16062826.

Ansari, A.M., Memon, L.A., Selim, M.Y.E., 2024. Experimental study of particulate matter emission for a diesel engine fueled with nanoparticles and biofuel/diesel blends. International Journal of Thermofluids 23, 100738. https://doi.org/10.1016/j.ijft.2024.100738.

Bisig, C., Steiner, S., Comte, P., Czerwinski, J., Mayer, A., Petri-Fink, A., et al., 2015. Biological effects in lung cells in vitro of exhaust aerosols from a gasoline passenger car with and without particle filter. Emiss. Control Sci. Technol. 1, 237–246. https://doi.org/10.1007/s40825-015-0019-6.

Bortnowski, P., Matla, J., Sierzputowski, G., Włostowski, R., Wróbel, R., 2024. Prediction of toxic compounds emissions in exhaust gases based on engine vibration and Bayesian optimized decision trees. Measurement 235, 115018. https://doi.org/10.1016/j.measurement.2024.115018.

Botero, M.L., Mendoza, C., Arias, S., Hincapié, O.D., Agudelo, J.R., Ortiz, I.C., 2020. In vitro evaluation of the cytotoxicity, mutagenicity and DNA damage induced by particle matter and gaseous emissions from a medium-duty diesel vehicle under real driving conditions using palm oil biodiesel blends. Environ. Pollut. 265, 115034. https://doi.org/10.1016/j.envpol.2020.115034.

Cattani-Cavalieri, I., Trombetta-Lima, M., Yan, H., Manzano-Covarrubias, A.L., Baarsma, H.A., Oun, A., van der Veen, M.M., Oosterhout, E., Dolga, A.M., Ostrom, R. S., Valenca, S.S., Schmidt, M., 2024. Diesel exhaust particles alter mitochondrial bioenergetics and cAMP producing capacity in human bronchial epithelial cells. Front. Toxicol. 6, 1412864. https://doi.org/10.3389/ftox.2024.1412864.

Chakraborty, J., Caicci, F., Roy, M., Ziviani, E., 2020. Investigating mitochondrial autophagy by routine transmission electron microscopy: seeing is believing? Pharmacol. Res. 160, 105097. https://doi.org/10.1016/j.phrs.2020.105097.

Chen, Y., Li, Y., Gu, W., Long, Y., Wang, Y., Zhang, H., et al., 2025. A putative adverse outcome pathway linking diesel engine exhaust with increased risks of metabolism-related diseases: a metabolomics-based molecular epidemiology study. Environ. Technol. Innov. 38, 104116. https://doi.org/10.1016/j.eti.2025.104116.

Cole, N.B., Daniels, M.P., Levine, R.L., Kim, G., 2010. Oxidative stress causes reversible changes in mitochondrial permeability and structure. Exp. Gerontol. 45, 596–602. https://doi.org/10.1016/j.exger.2010.01.016.

Collins, H.E., Kane, M.S., Litovsky, S.H., Darley-Usmar, V.M., Young, M.E., Chatham, J. C., Zhang, J., 2021. Mitochondrial morphology and mitophagy in heart diseases: qualitative and quantitative analyses using transmission electron microscopy. Front. Aging 2, 670267. https://doi.org/10.3389/fragi.2021.670267.

Darzynkiewicz, Z., Halicka, H.D., Zhao, H., 2010. Analysis of cellular DNA content by flow and laser scanning. Cytometry 137–147. https://doi.org/10.1007/978-1-4419-6199-0_9.

de Albuquerque, P.B.S., Rodrigues, N.E.R., Silva, P.M. dos S., de Oliveira, W.F., Correia, M.T. dos S., Coelho, L.C.B.B., 2023. The use of proteins, lipids, and carbohydrates in the management of wounds. Molecules 28 (4), 1580. https://doi.org/10.3390/molecules28041580.

Drizik, E., Corbett, S., Zheng, Y., Vermeulen, R., Dai, Y., Hu, W., et al., 2020. Transcriptomic changes in the nasal epithelium associated with diesel engine exhaust exposure. Environ. Int. 137, 105506. https://doi.org/10.1016/j.envint.2020.105506.

Fu, J., Fang, T., Gao, Y., Wang, T., Jia, Z., Guo, D., et al., 2024. Emission characteristic, spatial distribution, and health risk of polycyclic aromatic compounds (PAHs, NPAHs, and OPAHs) from light-duty gasoline and diesel vehicles based on on-road measurements. Sci. Total Environ. 941, 173390. https://doi.org/10.1016/j.scitotenv.2024.173390.

ISO-10993:5, Biologiczna ocena wyrobów medycznych – Część 5: Badania cytotoksyczności in vitro. n.d.

Janicka, A., 2013. Ocena toksyczności mikroatmosfery środowiska wnętrza pojazdu samochodowego. Oficyna Wydawnicza Politechniki Wrocławskiej, Wrocław.

Jendrach, M., Mai, S., Pohl, S., Vöth, M., Bereiter-Hahn, J., 2008. Short- and long-term alterations of mitochondrial morphology, dynamics and mtDNA after transient oxidative stress. Mitochondrion 8, 293–304. https://doi.org/10.1016/j.mito.2008.06.001.

Kale, A.V., Krishnasamy, A., 2024. Experimental study on combustion, performance, and emission characteristics of a homogeneous charge compression ignition engine fuelled with multiple biofuel-gasoline blends. Energy 288, 129621. https://doi.org/10.1016/j.energy.2023.129621.

Kęska, A., 2023. The actual toxicity of engine exhaust gases emitted from vehicles: the development and perspectives of biological and chemical measurement methods. ACS Omega 8, 24718–24726. https://doi.org/10.1021/acsomega.3c02171.

Kęska, A., Janicka, A., Zawiślak, M., Molska, J., Włostowski, R., Włóka, A., et al., 2022. Assessment of the actual toxicity of engine exhaust gas emissions from Euro 3 and Euro 6 compliant vehicles with the BAT-CELL method using in vitro tests. Int. J. Environ. Res. Public Health 19, 14138. https://doi.org/10.3390/ijerph192114138.

Kęska, A., Janicka, A., Zawiślak, M., 2023. Numerical optimization of the BAT-CELL Bio-Ambient-Tests method for engine exhausts toxicity evaluation. Combustion Engines 192, 19–25. https://doi.org/10.19206/CE-147781.

Kęska, A., Rusak, A., Włostowski, R., Dziemieszkiewicz, M., Szymlet, N., 2024. Low-vacuum SEM imaging and viability test of L929 cells exposed to a Euro 6 diesel exhaust gas mixture in a BAT-CELL chamber in comparison with hydrocarbons emission. Sci. Rep. 14, 12883. https://doi.org/10.1038/s41598-024-63560-4.

Koman, G., Kubina, M., Varmus, M., 2024. Electromobility in the world and in Slovakia. Transportation Research Procedia 77, 224–230. https://doi.org/10.1016/j.trpro.2024.01.030.

Kumar, V., Behera, S.N., 2024. Characterization of trace elements of size-resolved particulate matter, development of emission factors and human health impacts associated with stationary diesel engine exhausts. Journal of Hazardous Materials Advances 14, 100432. https://doi.org/10.1016/j.hazadv.2024.100432.

Landwehr, K.R., Hillas, J., Mead-Hunter, R., Brooks, P., King, A., O'Leary, R.A., et al., 2021. Fuel feedstock determines biodiesel exhaust toxicity in a human airway epithelial cell exposure model. J. Hazard. Mater. 420, 126637. https://doi.org/10.1016/j.jhazmat.2021.126637.

Li, J., Cheng, T., Wu, H., Yang, L., 2023. Hydrophobic carbon with hollow and hierarchical porous structures for efficient VOCs removal from complex exhaust gases: experiments and DFT calculations. Chem. Eng. J. 478, 147290. https://doi.org/10.1016/j.cej.2023.147290.

Li, Z., Zhang, W., Pang, C., Mao, S., Chen, Z., Chen, S., et al., 2024. Developing and validating a tailored olefins kinetics model for reducing unregulated pollutant emissions in diesel engines. Fuel 374, 132391. https://doi.org/10.1016/j.fuel.2024.132391.

Mandal, P., 2017. Potential biomarkers associated with oxidative stress for risk assessment of colorectal cancer. Naunyn Schmiedeberg's Arch. Pharmacol. 390, 557–565. https://doi.org/10.1007/s00210-017-1352-9.

McDonald, P.C., Nagel, J.M., Dedhar, S., 2021. Anastasis, recovery from the brink of death as a mechanism of drug resistance. In: Biological Mechanisms and the Advancing Approaches to Overcoming Cancer Drug Resistance. Elsevier, pp. 251–260. https://doi.org/10.1016/B978-0-12-821310-0.00004-8.

Mosieniak, G., Sliwinska, M.A., Alster, O., Strzeszewska, A., Sunderland, P., Piechota, M., et al., 2015. Polyploidy formation in doxorubicin-treated cancer cells can favor escape from senescence. Neoplasia 17, 882–893. https://doi.org/10.1016/j.neo.2015.11.008.

Nabi, M.N., Rasul, M.G., Hazrat, M.A., Rashid, F., 2024. Investigation of the effect of ether oxygenated additives on diesel engine performance, combustion, and exhaust emissions - an experimental approach. Energy 304, 132223. https://doi.org/10.1016/j.energy.2024.132223.

Niu, X., Chuang, H.-C., Wang, X., Ho, S.S.H., Li, L., Qu, L., et al., 2020. Cytotoxicity of PM2.5 vehicular emissions in the Shing Mun Tunnel, Hong Kong. Environ. Pollut. 263, 114386. https://doi.org/10.1016/j.envpol.2020.114386.

Paduch, R., 2019. Praktikum z hodowli komórek i tkanek. Wydawnictwo Uniwersytetu Marii Curie-Skłodowskiej, Lublin.

Rahman Adib, A., Mizanur Rahman, Md, Hassan, T., Ahmed, M., Al Rifat, A., 2024. Novel biofuel blends for diesel engines: optimizing engine performance and emissions with *C. cohnii* microalgae biodiesel and algae-derived renewable diesel blends. Energy Conversion and Management: X 23, 100688. https://doi.org/10.1016/j.ecmx.2024.100688.

Scholten, R.H., Essig, Y.J., Roursgaard, M., Jensen, A., Krais, A.M., Gren, L., et al., 2021. Inhalation of hydrogenated vegetable oil combustion exhaust and genotoxicity responses in humans. Arch. Toxicol. 95, 3407–3416. https://doi.org/10.1007/s00204-021-03143-8.

Sivakumar, B., Kurian, G.A., 2022. Inhalation of PM $_{2.5}$ from diesel exhaust promote impairment of mitochondrial bioenergetics and dysregulate mitochondrial quality in rat heart: implications in isoproterenol-induced myocardial infarction model. Inhal. Toxicol. 34, 107–119. https://doi.org/10.1080/08958378.2022.2049931.

Solarska-Ściuk, K., Adach, K., Fijałkowski, M., Haczkiewicz-Leśniak, K., Kulus, M., Olbromski, M., et al., 2022. Identifying the molecular mechanisms and types of cell death induced by bio- and pyr-silica nanoparticles in endothelial cells. Int. J. Mol. Sci. 23, 5103. https://doi.org/10.3390/ijms23095103.

Steiner, S., Bisig, C., Petri-Fink, A., Rothen-Rutishauser, B., 2016. Diesel exhaust: current knowledge of adverse effects and underlying cellular mechanisms. Arch. Toxicol. 90, 1541–1553. https://doi.org/10.1007/s00204-016-1736-5.

Wan, F., Zhong, G., Ning, Z., Liao, J., Yu, W., Wang, C., et al., 2020. Long-term exposure to copper induces autophagy and apoptosis through oxidative stress in rat kidneys. Ecotoxicol. Environ. Saf. 190, 110158. https://doi.org/10.1016/j.ecoenv.2019.110158.

Wu, H.-H., Zhu, Q., Liang, N., Xiang, Y., Xu, T.-Y., Huang, Z.-C., Cai, J.Y., Weng, L.L., Ge, H.S., 2024. *CISD2* regulates oxidative stress and mitophagy to maintain the balance of the follicular microenvironment in PCOS. Redox Rep. 29 (1), 2377870. https://doi.org/10.1080/13510002.2024.2377870.

Yu, S., Zhu, W., Yu, L., 2024. The role of rapamycin in the PINK1/Parkin signaling pathway in mitophagy in podocytes. Open Life Sci. 19 (1), 20220958. https://doi.org/10.1515/biol-2022-0958.

Zawadzka-Knefel, A., Rusak, A., Mrozowska, M., Machałowski, T., Żak, A., Haczkiewicz-Leśniak, K., Kulus, Michał, Kuropka, Piotr, Podhorska-Okołów, Marzenna, Skośkiewicz-Malinowska, Katarzyna, 2023. Chitin scaffolds derived from the marine demosponge *Aplysina fistularis* stimulate the differentiation of dental pulp stem cells. Front. Bioeng. Biotechnol. 11, 1254506. https://doi.org/10.3389/fbioe.2023.1254506.

Zerboni, A., Rossi, T., Bengalli, R., Catelani, T., Rizzi, C., Priola, M., et al., 2022. Diesel exhaust particulate emissions and in vitro toxicity from Euro 3 and Euro 6 vehicles. Environ. Pollut. 297, 118767. https://doi.org/10.1016/j.envpol.2021.118767.

Zhang, Y., Deng, W., Hu, Q., Wu, Z., Yang, W., Zhang, H., et al., 2020. Comparison between idling and cruising gasoline vehicles in primary emissions and secondary organic aerosol formation during photochemical ageing. Sci. Total Environ. 722, 137934. https://doi.org/10.1016/j.scitotenv.2020.137934.